

# DreamWaltz: Make a Scene with Complex 3D Animatable Avatars

**Yukun Huang<sup>1,2</sup>, Jianan Wang<sup>2</sup>, Ailing Zeng<sup>2</sup>, He Cao<sup>2</sup>, Xianbiao Qi<sup>2</sup>, Yukai Shi<sup>2</sup>,  
Zheng-Jun Zha<sup>1</sup>, Lei Zhang<sup>2</sup>**

<sup>1</sup>University of Science and Technology of China

<sup>2</sup>International Digital Economy Academy (IDEA)

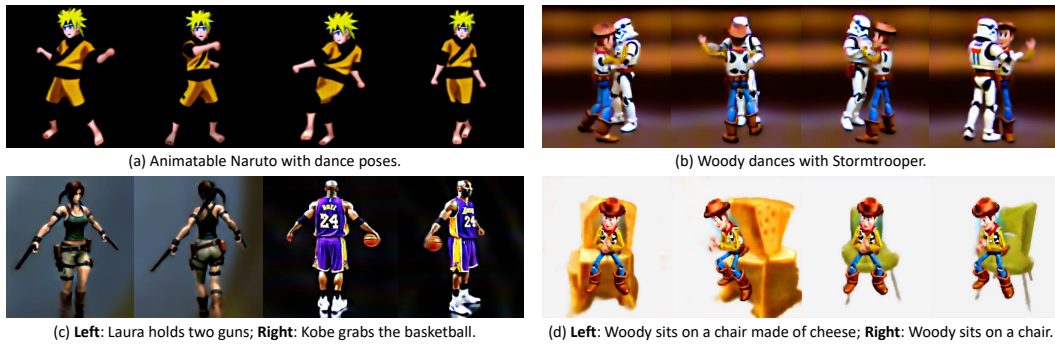


Figure 1: DreamWaltz focuses on text-to-avatar creation, which can (a) create animatable avatars, (b-d) make a complex 3D scene with diverse interactions (b) across avatars, (c) between avatar and objects or (d) between avatar and the scene without retraining.

## Abstract

We present DreamWaltz, a novel framework for generating and animating complex avatars given text guidance and parametric human body prior. While recent methods have shown encouraging results in the text-to-3D generation of common objects, creating high-quality and animatable 3D avatars remains challenging. To create high-quality 3D avatars, DreamWaltz proposes 3D-consistent occlusion-aware Score Distillation Sampling (SDS) to optimize implicit neural representations with canonical poses. It provides view-aligned supervision via 3D-aware skeleton conditioning and enables complex avatar generation without artifacts and multiple faces. For animation, our method learns an animatable and generalizable avatar representation which could map arbitrary poses to the canonical pose representation. Extensive evaluations demonstrate that DreamWaltz is an effective and robust approach for creating 3D avatars that can take on complex shapes and appearances as well as novel poses for animation. The proposed framework further enables the creation of complex scenes with diverse compositions, including avatar-avatar, avatar-object and avatar-scene interactions.

## 1 Introduction

The creation and animation of 3D digital avatars are essential for various applications, including film and cartoon production, video game design, and immersive media such as AR and VR. However, traditional techniques for constructing such intricate 3D models are costly and time-consuming, requiring thousands of hours from skilled artists with extensive aesthetics and 3D modeling knowledge.

<sup>1</sup>This work was done when Yukun was intern at IDEA.

In this work, we seek a solution for 3D avatar generation that satisfies the following desiderata: (1) easily controllable over avatar properties through textual descriptions; (2) capable of producing high-quality and diverse 3D avatars with complex shapes and appearances; (3) the generated avatars should be ready for animation and scene composition with diverse interactions.

The advancement of deep learning methods has enabled promising methods which can reconstruct 3D human models from monocular images [33, 41] or videos [40, 13, 42, 38, 11, 27]. Nonetheless, these methods rely heavily on the strong visual priors from image/video and human body geometry, making them unsuitable for generating creative avatars that can take on complex and imaginative shapes or appearances. Recently, integrating 2D generative models into 3D modeling [28, 15] has gained significant attention to make 3D digitization more accessible, reducing the dependency on extensive 3D datasets. However, creating animatable 3D avatars remains challenging: Firstly, avatars often require intricate and complex details for their appearance (e.g., loose cloth, diverse hair, and different accessories); secondly, avatars have articulated structures where each body part is able to assume various poses in a coordinated and constrained way; and thirdly, avatar changes shape and texture details such as creases when assuming different poses, making animation for complex avatars extremely challenging. As a result, while DreamFusion [28] and subsequent methods [15, 5] demonstrate impressive results on text-guided creation of stationary everyday objects, they lack the proper constraints to enforce consistent 3D avatar structures and appearances, with difficulties in producing intricate shapes, appearances and poses for 3D avatars, let alone for animation.

In this paper, we present DreamWaltz, a framework for generating high-quality 3D digital avatars from text prompts, body shapes, and poses, ready for animation and composition with diverse avatar-avatar, avatar-object and avatar-scene interactions. DreamWaltz employs a trainable Neural Radiance Field (NeRF) as the 3D avatar representation, a pre-trained text-and-skeleton-conditional diffusion model [44] for shape and appearance supervision, and SMPL models [2] for extracting 3D-aware posed-skeletons. Our method enables high-quality avatar generation with 3D-consistent SDS, which resolves the view disparity between the diffusion model’s supervision image and NeRF’s rendering. By training an animatable and generalizable NeRF with sampled human pose prior, we can deform the generated avatar to arbitrary poses for realistic animation without retraining.

The key contributions of DreamWaltz lie in four main aspects:

- We propose a novel 3D animatable avatar generation framework named DreamWaltz, for the first time capable of generating avatars with complex shapes and appearances, ready for high-quality animation and interaction.
- For avatar creation, we propose a text-guided 3D-consistent score distillation sampling strategy (SDS) with occlusion culling, enabling the generation of high-quality avatars, e.g., avoiding the Janus (multi-face) problem and pose ambiguity.
- We propose to learn an animatable and generalizable NeRF representation with sampled human pose prior, which enables the animation of complex avatars. Once trained, we can generate any motion sequence of the created avatar without retraining.
- Benefiting from DreamWaltz, we can make a scene with diverse interactions across avatars, objects, and scenes. We conduct extensive experiments and show that DreamWaltz is effective and robust in creating complex, high-quality 3D avatars ready for realistic animation and interaction.

## 2 Related Work

**Text-guided image generation.** Recently, there have been significant advancements in text-to-image models such as GLIDE [23], unCLIP [30], Imagen [32], and Stable Diffusion [31], which enable the generation of highly realistic and imaginative images based on text prompts. These generative capabilities have been made possible by advancements in modeling, such as diffusion models [6, 36, 24], and the availability of large-scale web data containing billions of image-text pairs [34, 35, 4]. These datasets encompass a wide range of general objects, with significant variations in color, texture, and camera viewpoints, providing pre-trained models with a comprehensive understanding of general objects and enabling the synthesis of high-quality and diverse objects. Furthermore, recent works [44, 9, 14] have explored incorporating additional conditioning, such as depth maps and human skeleton poses, to generate images with more precise control.

	Complex (non-skin-tight)	Animatable	Interactive (avatar-avatar/object/scene)
AvatarCLIP [8]	✗	✓	✗
AvatarCraft [12]	✗	✓	✗
DreamAvatar [3]	✓	✗	✗
DreamWaltz (Ours)	✓	✓	✓

Table 1: Comparison of 3D avatar generation methods, including the complexity of avatar shape and appearance, animation, and demonstration of scene composition with diverse interactions.

**Text-guided 3D generation.** Dream Fields [10] and CLIPmesh [20] were groundbreaking in their utilization of CLIP [29] to optimize an underlying 3D representation, aligning its 2D renderings with user-specified text prompts, without necessitating costly 3D training data. However, this approach tends to result in less realistic 3D models since CLIP only provides discriminative supervision for high-level semantics. In contrast, recent works have demonstrated remarkable text-to-3D generation results by employing powerful text-to-image diffusion models as a robust 2D prior to optimizing a trainable NeRF with Score Distillation Sampling (SDS) [28, 15, 5]. Nonetheless, the produced geometry and texture are static, blurry and usually lack intricate details necessary for avatar creation.

**Text-guided 3D avatar generation.** Avatar-CLIP [8] starts with initializing 3D human geometry via a shape VAE network and subsequently employs CLIP [29] for shape sculpting and texture generation. To animate the generated 3D avatar, they propose a CLIP-guided reference-based motion synthesis method. However, this approach tends to produce less realistic and oversimplified 3D models since CLIP only provides discriminative guidance on high-level semantics. Concurrent to our work, DreamAvatar [3] and AvatarCraft [12] both utilize pre-trained text-to-image diffusion models and SMPL models as shape prior for avatar generation. While DreamAvatar focuses on producing static posed-3D avatars which are incapable of animation, AvatarCraft generates higher-quality avatars via coarse-to-fine and multi-box training and enables animation via local transformation between the template mesh and the target mesh based on SMPL models. However, due to heavy reliance on SMPL prior, AvatarCraft is limited to generating avatars that closely resemble bare humans (skin-tight). In contrast, we utilize SMPL models as a weak prior for initialization and to prompt 2D generative models with 3D-aware poses, which are flexible in generating complex avatars. For animation, we propose learning a generalizable deformation field between the canonical pose and any target pose based on randomly sampled SMPL models. This approach facilitates effortless manipulation of the avatar’s pose and allows for realistic interactions between generated avatars, objects, and the scene. We summarize the key differences between our work and related works in Table 1.

### 3 Method

#### 3.1 Preliminary

**Text-to-3D generation.** Recent methods [28, 15, 18] have shown encouraging results on text-to-3D generation of common objects by integrating three essential components:

(1) *Neural Radiance Fields* (NeRF) [22, 1, 19] is commonly adopted as the 3D representation for text-to-3D generation [37, 15], parameterized by a trainable MLP. For rendering, a batch of rays  $\mathbf{r}(k) = \mathbf{o} + \mathbf{k}\mathbf{d}$  are sampled based on the camera position  $\mathbf{o}$  and direction  $\mathbf{d}$  on a per-pixel basis. The MLP takes  $\mathbf{r}(k)$  as input and predicts density  $\tau$  and color  $c$ . The volume rendering integral is then approximated using numerical quadrature to yield the final color of the rendered pixel:

$$\hat{C}_c(\mathbf{r}) = \sum_{i=1}^{N_c} \Omega_i \cdot (1 - \exp(-\tau_i \delta_i)) c_i,$$

where  $N_c$  is the number of sampled points on a ray,  $\Omega_i = \exp(-\sum_{j=1}^{i-1} \tau_j \delta_j)$  is the accumulated transmittance, and  $\delta_i$  is the distance between adjacent sample points.

(2) *Diffusion models* [7, 24] which have been pre-trained on extensive image-text datasets [30, 32, 37] provide a robust image prior for supervising text-to-3D generation. Diffusion models learn to

estimate the denoising score  $\nabla_{\mathbf{x}} \log p_{\text{data}}(\mathbf{x})$  by adding noise to clean data  $\mathbf{x} \sim p(\mathbf{x})$  (forward process) and learning to reverse the added noise (backward process). Noising the data distribution to isotropic Gaussian is performed in  $T$  timesteps, with a pre-defined noising schedule  $\alpha_t \in (0, 1)$  and  $\bar{\alpha}_t := \prod_{s=1}^t \alpha_s$ , according to:

$$\mathbf{z}_t = \sqrt{\bar{\alpha}_t} \mathbf{x} + \sqrt{1 - \bar{\alpha}_t} \boldsymbol{\epsilon}, \text{ where } \boldsymbol{\epsilon} \sim \mathcal{N}(\mathbf{0}, \mathbf{I}).$$

In the training process, the diffusion models learn to estimate the noise by

$$\mathcal{L}_t = \mathbb{E}_{\mathbf{x}, \boldsymbol{\epsilon} \sim \mathcal{N}(\mathbf{0}, \mathbf{I})} \left[ \|\boldsymbol{\epsilon}_\phi(\mathbf{z}_t, t) - \boldsymbol{\epsilon}\|_2^2 \right].$$

Once trained, one can estimate  $\mathbf{x}$  from noisy input and the corresponding noise prediction.

(3) *Score Distillation Sampling* (SDS) [28, 15, 18] is a technique introduced by DreamFusion [28] and extensively employed to distill knowledge from a pre-trained diffusion model  $\boldsymbol{\epsilon}_\phi$  into a differentiable 3D representation. For a NeRF model parameterized by  $\boldsymbol{\theta}$ , its rendering  $\mathbf{x}$  can be obtained by  $\mathbf{x} = g(\boldsymbol{\theta})$  where  $g$  is a differentiable renderer. SDS calculates the gradients of NeRF parameters  $\boldsymbol{\theta}$  by,

$$\nabla_{\boldsymbol{\theta}} \mathcal{L}_{\text{SDS}}(\boldsymbol{\phi}, \mathbf{x}) = \mathbb{E}_{t, \boldsymbol{\epsilon}} \left[ w(t) (\boldsymbol{\epsilon}_\phi(\mathbf{x}_t; y, t) - \boldsymbol{\epsilon}) \frac{\partial \mathbf{z}_t}{\partial \mathbf{x}} \frac{\partial \mathbf{x}}{\partial \boldsymbol{\theta}} \right], \quad (1)$$

where  $w(t)$  is a weighting function that depends on the timestep  $t$  and  $y$  denotes the given text prompt.

(3) *SMPL* [16] is a 3D parametric human body model with a vertex-based linear model, which decomposes body deformation into identity-related and pose-related shape deformation. It contains  $N = 6,890$  vertices and  $K = 24$  keypoints. Benefiting from its efficient and expressive human motion representation ability, SMPL has been widely used in human motion-driven tasks [8, 43, 17]. SMPL parameters include a 3D body joint rotation  $\boldsymbol{\xi} \in \mathbb{R}^{K \times 3}$ , a body shape  $\boldsymbol{\beta} \in \mathbb{R}^{10}$ , and a 3D global scale and translation  $t \in \mathbb{R}^3$ .

Formally, constructing a rest pose  $T(\boldsymbol{\beta}, \boldsymbol{\xi})$  involves combining the mean template shape  $\bar{T}$  from the canonical space, the shape-dependent deformations  $B_S(\boldsymbol{\beta}) \in \mathbb{R}^{3N}$ , and the pose-dependent deformations  $B_P(\boldsymbol{\xi}) \in \mathbb{R}^{3N}$  to relieve artifacts in a standard linear blend skinning (LBS) [21] by,

$$T(\boldsymbol{\beta}, \boldsymbol{\xi}) = \bar{T} + B_S(\boldsymbol{\beta}) + B_P(\boldsymbol{\xi}).$$

To map the SMPL parameters  $\boldsymbol{\beta}, \boldsymbol{\xi}$  to a triangulated mesh, a function  $M$  is adopted to combine the rest pose mesh  $T(\boldsymbol{\beta}, \boldsymbol{\xi})$ , the corresponding keypoint positions  $\mathcal{J}(\boldsymbol{\beta}) \in \mathbb{R}^{3K}$ , pose  $\boldsymbol{\xi}$ , and a set of blend weights  $\mathcal{W} \in \mathbb{R}^{N \times K}$  via a LBS function as,

$$M(\boldsymbol{\beta}, \boldsymbol{\xi}) = W(T(\boldsymbol{\beta}, \boldsymbol{\xi}), \mathcal{J}(\boldsymbol{\beta}), \boldsymbol{\xi}, \mathcal{W}).$$

To obtain the corresponding vertex under the observation pose  $\mathbf{v}_o$ , we use an affine deformation  $\mathcal{G}_k(\boldsymbol{\xi}, j_k)$  with skinning weight  $w_k$  to transform the  $k_{th}$  keypoint  $j_k$  from the canonical pose to the observation pose as,

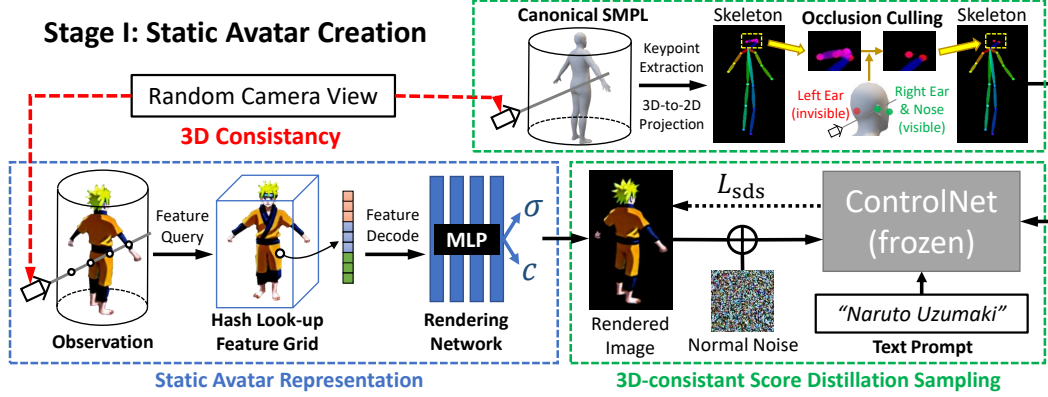
$$\mathbf{v}_o = \sum_{k=1}^K w_k \mathcal{G}_k(\boldsymbol{\xi}, j_k). \quad (2)$$

## 3.2 DreamWaltz: Make a Scene with Complex 3D Animatable Avatars

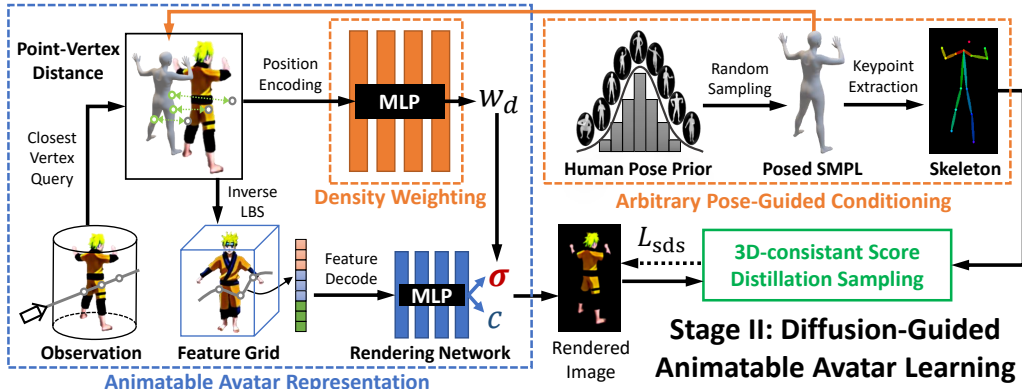
### 3.2.1 Creating a Static Avatar

DreamWaltz employs a trainable NeRF as the 3D avatar representation. It leverages SMPL prior in two ways: (1) initializing NeRF; (2) extracting 3D-aware and occlusion-aware posed-skeletons to condition ControlNet [44] for 3D-consistent Score Distillation Sampling. Fig 2 (a) illustrates our method on how to create a static avatar.

**SMPL-guided Initialization.** To speed up the NeRF optimization and to provide a reasonable initial input for the diffusion model, we pre-train NeRF based on an SMPL mesh. The SMPL model could be in the canonical pose as adopted in our method to avoid self-occlusion or in any chosen pose for posed-avatar creation [3]. Specifically, we render the silhouette image  $x_{\text{sil}}$  of the SMPL model given a randomly sampled viewpoint and minimize the MSE loss between the NeRF-rendered



(a) **Static Avatar Creation.** During SDS optimization, we randomly sample a camera viewpoint to render both the 3D avatar and an SMPL model. The extracted SMPL keypoints are projected to a 2D skeleton image with further occlusion culling. The skeleton image is by construction 3D-consistent with the rendered avatar. We then utilize ControlNet [44] conditioned on the text prompt and the skeleton image instead of the original SD [31].



(b) **Animatable Avatar Learning.** During training, we randomly sample SMPL models of viable poses to condition ControlNet [44] and to learn a generalizable density weighting function to refine vertex-based pose transformation, enabling animation of complex avatars.

Figure 2: Illustration of our framework for static and animatable avatar creation. (a) shows how to create a static avatar, and (b) demonstrates how to learn an animatable avatar.

image  $x$  and the silhouette image  $x_{\text{sil}}$ . Note that our NeRF renders images in the latent space of Stable Diffusion [31], so it is necessary to use the VAE-based image encoder to transform silhouette images into the latent space for the loss calculation. We empirically found that SMPL-guided NeRF initialization significantly improves the geometry and the convergence speed for avatar generation.

**3D-consistent Score Distillation Sampling.** Vanilla SDS [37, 39, 15] as previously introduced in Sec. 3.1 utilizes view-dependent prompt augmentations such as “front view of ...” for diffusion model to provide crucial 3D view-consistent supervision. However, this prompting strategy cannot guarantee precise view consistency, leaving the disparity between the viewpoint of the diffusion model’s supervision image and NeRF’s rendering image unresolved. Such inconsistency causes quality issues for 3D generation, such as blurriness and the Janus (multi-face) problem. Inspired by recent works of controllable image generation [44, 14], we propose to utilize additional 3D-aware conditioning images to improve SDS for 3D-consistent NeRF optimization. Specifically, additional conditioning image  $c$  is injected to Eq. 1 for SDS gradient computation:

$$\nabla_{\theta} \mathcal{L}_{\text{SDS}}(\phi, \mathbf{x}) = \mathbb{E}_{t, \epsilon} \left[ w(t)(\epsilon_{\phi}(\mathbf{x}_t; y, t, c) - \epsilon) \frac{\partial \mathbf{z}_t}{\partial \mathbf{x}} \frac{\partial \mathbf{x}}{\partial \theta} \right], \quad (3)$$

where conditioning image  $c$  can be one or a combination of skeletons, depth maps, normal maps and etc. In practice, we choose skeletons as the conditional image type because they provide minimal image structure priors and enable complex avatar generation. In order to acquire 3D-consistent

supervision, the conditioning image’s viewpoint should be in sync with NeRF’s rendering viewpoint. To achieve this for avatar generation, we use human SMPL models to produce conditioning images.

**Occlusion Culling.** The introduction of 3D-aware conditional images can enhance the 3D consistency in the SDS optimization process. However, the effectiveness is constrained by the adopted diffusion model [44] on its interpretation of the conditional images. As shown in Fig. 7 (a), we provide a back-view skeleton map as the conditional image to ControlNet [44] and perform text-to-image generation, but a frontal face still appears in the generated image. Such defects bring problems such as multiple faces and unclear facial features to 3D avatar generation. To this end, we propose to use occlusion culling algorithms [25] in computational graphics to detect whether facial keypoints are visible from the given viewpoint and subsequently remove them from the skeleton map if considered invisible. Body keypoints remain unaltered because they reside in the SMPL mesh, and it is difficult to determine whether they are occluded without introducing new priors.

### 3.2.2 Learning an Animatable Avatar

Figure 2 (b) shows our framework for generating animatable 3D avatars. In the training process, we randomly sample SMPL models of viable poses to condition ControlNet [44] and learn a generalizable density weighting function to refine vertex-based pose transformation, enabling animation of complex avatars. At test time, DreamWaltz is capable of creating an animation based on arbitrary motion sequences *without requiring further pose-by-pose retraining*.

**SMPL-guided Avatar Articulation.** Referring to Sec. 3.1, SMPL defines a vertex transformation from observation space to canonical space according to Eq. 2. In this work, we use SMPL-guided transformation to achieve NeRF-represented avatar articulation. More concretely, for each sampled point  $\mathbf{p}$  on a NeRF ray, we find its closest vertex  $\mathbf{v}_c$  based on a posed SMPL mesh. We then utilize the transformation matrix  $\mathbf{T}_{\text{skel}}$  of  $\mathbf{v}_c$  to project  $\mathbf{p}$  to the canonical space feature grid for feature querying and subsequent volume rendering. When  $\mathbf{p}$  is close to  $\mathbf{v}_c$ , the calculated articulation is approximately correct. However, for non-skin-tight complex avatars,  $\mathbf{p}$  may be far away from any mesh vertex, resulting in erroneous coordinate transformation causing quality issues such as extra limbs and artifacts. To avoid such problems, we further introduce a novel density weighting mechanism.

**Density Weighting Network.** We propose a density weighting mechanism to suppress color contribution from erroneously transformed point  $\mathbf{p}$ , effectively alleviating undesirable artifacts. To achieve this, we train a generalizable density weighting network  $\text{MLP}_{\text{DRN}}$ . More concretely, we project sampled point  $\mathbf{p}$  and its closest vertex  $\mathbf{v}_c$  to canonical space via the transformation matrix  $\mathbf{T}_{\text{skel}}$ , embed these two coordinates with the positional embedding function  $\text{PE}(\cdot)$  and then use the concatenated embeddings as inputs to  $\text{MLP}_{\text{DRN}}$ . The process can be defined as,

$$d' = \text{MLP}_{\text{DRN}}(\text{PE}(\mathbf{T}_{\text{skel}} \cdot \mathbf{p}) \oplus \text{PE}(\mathbf{T}_{\text{skel}} \cdot \mathbf{v}_c)). \quad (4)$$

We then compute density weights  $w_d$  according to the distance  $d$  between  $\mathbf{p}$  and  $\mathbf{v}_c$ , and  $d'$ :

$$w_d = \text{Sigmoid}(-(d - d')/a). \quad (5)$$

where  $a$  is a preset parameter. Finally, the density  $\delta$  of sampled point  $\mathbf{p}$  is re-weighted to  $\delta \cdot w_d$  for subsequent volume rendering in NeRF.

**Sampled Human Pose Prior.** To enable animating generated avatars with arbitrary motion sequences, we need to make sure that the density weighting network  $\text{MLP}_{\text{DRN}}$  is generalizable to arbitrary poses. To achieve this, we utilize VPoser [26] as a human pose prior, which is a variational autoencoder that learns a latent representation of human pose. During training, we randomly sample SMPL pose parameters  $\xi$  from VPoser to construct the corresponding posed meshes. We utilize the mesh to (1) extract skeleton maps as conditioning images for 3D-consistent SDS; (2) to serve as mesh guidance for learning animatable avatar representation. This strategy aligns avatar articulation learning with SDS supervision, ensuring that  $\text{MLP}_{\text{DRN}}$  could learn a generalizable density weighting function from diverse poses. We also observe that SDS with diverse pose conditioning could further improve the visual quality of created avatar, e.g., sharper appearance.

### 3.2.3 Making a Complex 3D Scene via Diverse Interaction

DreamWaltz provides an effective solution to text-guided animatable avatar creation, readily applicable to make a scene with diverse interactions. For example, different animatable avatars could be

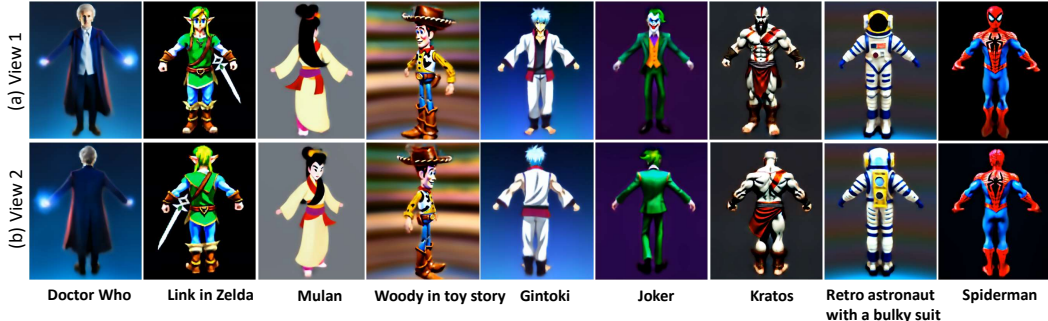


Figure 3: Qualitative results from two views of DreamWaltz. Given text prompts, it can generate high-quality 3D avatars with complex geometry and texture.

rendered in the same scene, achieving avatar-avatar animation. In Fig. 1 (b), we can make the avatar “Woody” dance with “Stormtrooper”. The animation process does not require any retraining. However, if the generated avatar exhibits any possible unruliness, artifacts, or interpenetration issues, we could use the introduced 3D-consistent SDS to further fine-tune the scene to improve the animation quality. Results will be provided in supplementary materials.

## 4 Experiment

We validate the effectiveness of our proposed framework for avatar generation and animation. In Sec. 4.1, we evaluate avatar generation with extensive text prompts for both qualitative comparisons and user studies. In Sec. 4.2, we evaluate avatar animation with two motion sequences. We demonstrate the efficacy of the proposed framework in making complex scenes with diverse interactions in Sec. 4.3. Finally, we present ablation analysis in Sec. 4.4.

**Implementation details.** DreamWaltz is implemented in PyTorch and can be trained and evaluated on a single NVIDIA 3090 GPU. For the static avatar creation stage, we train the avatar representation for 30,000 iterations, which takes about an hour. For the animatable avatar learning stage, the avatar representation and the introduced density weighting network are further trained for 50,000 iterations. Inference takes less than 3 seconds per rendering frame. Note that the two stages can be combined for joint training, but we decouple them for training efficiency.

### 4.1 Avatar Creation

#### 4.1.1 Qualitative Evaluations

**High-quality Avatar Generation.** We show 3D avatars created by DreamWaltz on diverse text prompts in Fig. 3. The geometry and texture quality are consistently high across different viewpoints for different text prompts.

**Comparison with SOTA methods.** We compare with existing SDS-based methods for complex (non-skin-tight) avatar generation. Latent-NeRF [18] and SJC [39] are general text-to-3D models. AvatarCraft [12] is not included for comparison because it cannot generate complex avatars. Furthermore, AvatarCraft utilizes a coarse-to-fine and body-face separated training to improve generation quality, which is orthogonal to our method. DreamAvatar [3] is the most relevant to our method, utilizing SMPL human prior without overly constraining avatar complexity. It is evident from Fig. 5 that our method consistently achieves higher quality in geometry and texture.

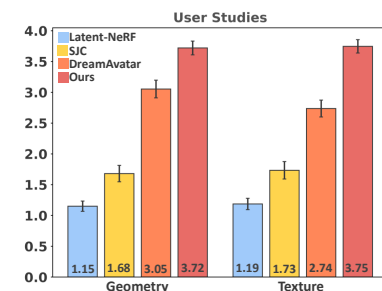


Figure 4: User preference study. DreamWaltz obtains higher scores in both geometry and texture.

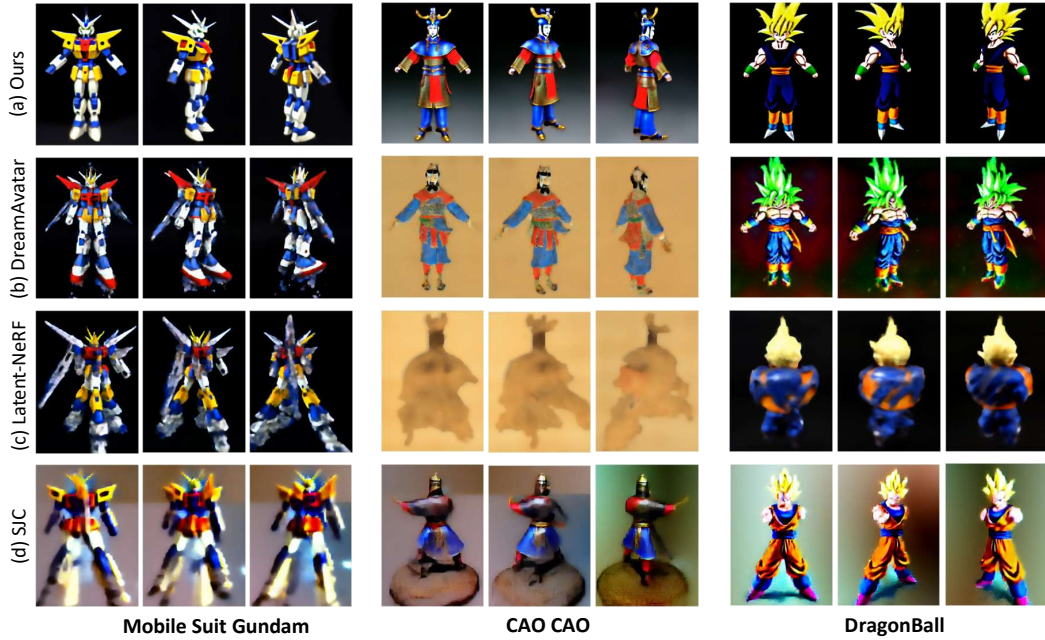


Figure 5: Qualitative comparisons for complex avatar generation. Text inputs are listed below.

#### 4.1.2 User Studies

We conduct user studies to evaluate the quality of avatar generation against Latent-NeRF [18], SJC [39] and DreamAvatar [3]. We use the 25 text prompts DreamAvatar released and their showcase models for comparison. We asked 12 volunteers to score 1 (worst) to 4 (best) in terms of (1) avatar geometry and (2) avatar texture. We do not measure text alignment as the avatar prompts are well-known characters universally respected by all the competing models. As shown in Fig. 4, the raters favor avatars generated by DreamWaltz for both better geometry and texture quality. Specifically, DreamWaltz outperforms DreamAvatar by score 0.67 on geometry and by score 1.01 on texture.

#### 4.2 Avatar Animation

We demonstrate the efficacy of our animation learning method with animation results on two motion sequences as shown in Fig. 6: row (a) displays motion sequences in skeletons as animation inputs; our framework directly apply the motion sequences to our generated avatars “Flynn Rider” and “Woody” without any retraining. We render the corresponding normal and RGB sequences in (b) and (c). In (d), we provide free-viewpoint rendering of a chosen sequence frame. Since we essentially infer a posed 3D avatar for each motion frame, the renderings are by construction 3D-consistent and we can creatively use the 3D model for novel-view video generation.

#### 4.3 Diverse Interaction

Benefiting from DreamWaltz, we could compose animatable avatars and other 3D assets into the same scene. We give a few examples to highlight the potential for enabling diverse interactions: (1) avatar-avatar interaction as shown in Fig. 1 (b) depicting “Woody” dancing with “Stromtrooper”; (2) avatar-object interaction as shown in Fig. 1 (c) with weapon and basketball; and (3) avatar-scene interaction as shown in Fig. 1 (d) with “Woody” sitting on different chairs. The interactions can be freely composed to make a dynamic scene. More results will be provided in supplementary materials.

#### 4.4 Ablation Studies

To evaluate the design choices of DreamWaltz, we ablate on the effectiveness of (1) occlusion culling and (2) animation learning. Occlusion culling is crucial for resolving view ambiguity, both for 2D

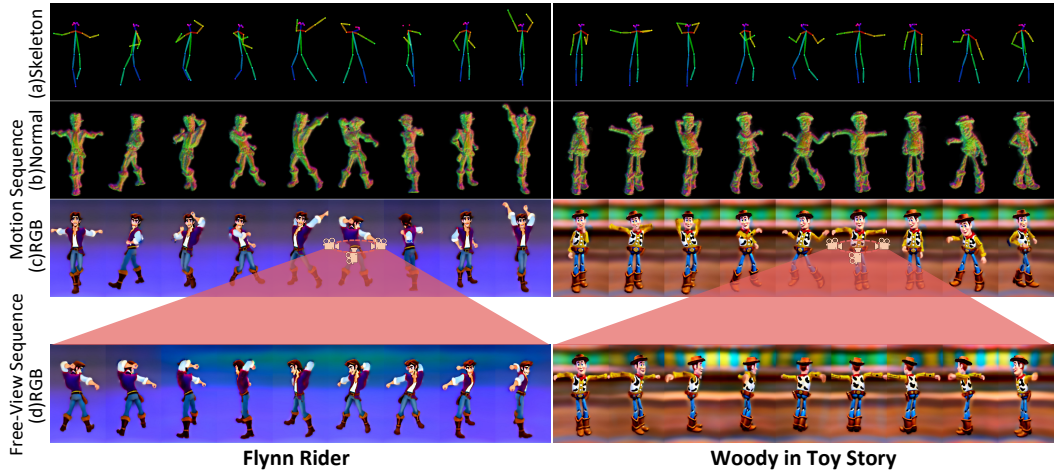


Figure 6: Animation results by applying skeleton motion sequences to animatable avatars generated by DreamWaltz. For each pose frame we could effortlessly render 3D-consistent free-viewpoints.

and 3D generation, as shown in Fig. 7 (a) and Fig. 7 (b), respectively. From Fig. 7 (c) it is evident that our animation learning method is significantly more effective than Inverse-LBS and AvatarCraft [12]. Note that AvatarCraft cannot faithfully animate complex features, e.g. Woody’s hat.

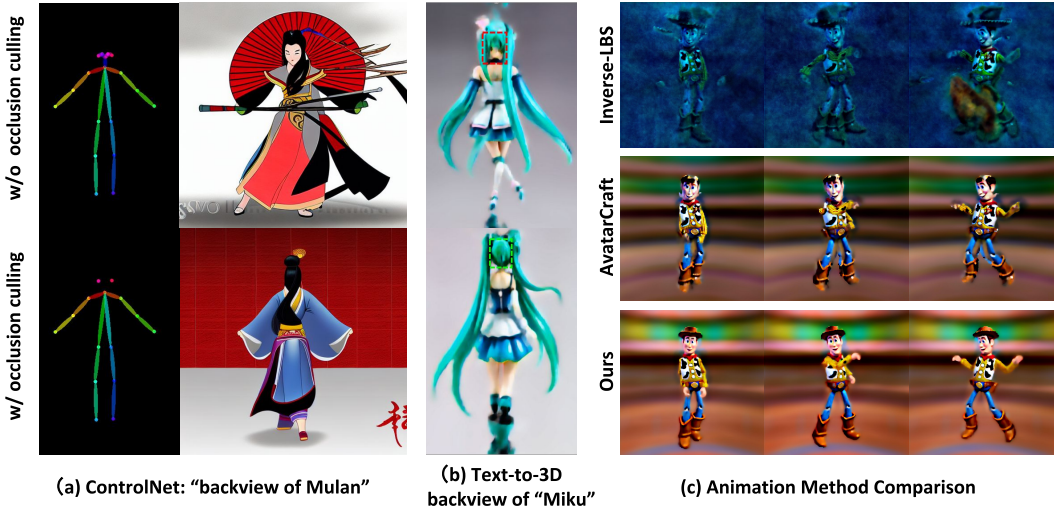


Figure 7: **Ablation Study.** Occlusion culling is crucial for view-consistency: it helps ControlNet [44] to correctly generate back view character (a), text-to-3D model to resolve the multi-face problem (b). Our proposed animation learning method empowers significantly higher-quality avatar animation (c).

## 5 Conclusion

We propose DreamWaltz, a novel learning framework for avatar creation and animation with text and shape guidance. For high-quality 3D avatar creation, we propose to leverage human priors with SMPL-guided initialization, further optimized with 3D-consistent occlusion-aware Score Distillation Sampling conditioned on 3D-aware skeletons. Our method learns an animatable and generalizable NeRF representation that could retarget the generated avatar to any pose, enabling realistic animation. Extensive experiments show that DreamWaltz is effective and robust with state-of-the-art avatar generation and animation. Benefiting from DreamWaltz, we could unleash our imagination and make diverse scenes with avatar-avatar, avatar-object, and avatar-scene interactions.

## References

- [1] Jonathan T Barron, Ben Mildenhall, Matthew Tancik, Peter Hedman, Ricardo Martin-Brualla, and Pratul P Srinivasan. Mip-NeRF: A Multiscale Representation for Anti-Aliasing Neural Radiance Fields. In *Proceedings of the IEEE/CVF International Conference on Computer Vision*, pages 5855–5864, 2021.
- [2] Federica Bogo, Angjoo Kanazawa, Christoph Lassner, Peter Gehler, Javier Romero, and Michael J Black. Keep it SMPL: Automatic estimation of 3D human pose and shape from a single image. In *Computer Vision–ECCV 2016: 14th European Conference, Amsterdam, The Netherlands, October 11–14, 2016, Proceedings, Part V 14*, pages 561–578. Springer, 2016.
- [3] Yukang Cao, Yan-Pei Cao, Kai Han, Ying Shan, and Kwan-Yee K Wong. DreamAvatar: Text-and-Shape Guided 3D Human Avatar Generation via Diffusion Models. *arXiv preprint arXiv:2304.00916*, 2023.
- [4] Soravit Changpinyo, Piyush Sharma, Nan Ding, and Radu Soricut. Conceptual 12M: Pushing Web-Scale Image-Text Pre-Training To Recognize Long-Tail Visual Concepts. In *Proceedings of the IEEE/CVF Conference on Computer Vision and Pattern Recognition*, pages 3558–3568, 2021.
- [5] Rui Chen, Yongwei Chen, Ningxin Jiao, and Kui Jia. Fantasia3D: Disentangling Geometry and Appearance for High-quality Text-to-3D Content Creation. *arXiv preprint arXiv:2303.13873*, 2023.
- [6] Prafulla Dhariwal and Alexander Nichol. Diffusion Models Beat GANs on Image Synthesis. *Advances in Neural Information Processing Systems*, 34:8780–8794, 2021.
- [7] Jonathan Ho, Ajay Jain, and Pieter Abbeel. Denoising Diffusion Probabilistic Models. *Advances in Neural Information Processing Systems*, 33:6840–6851, 2020.
- [8] Fangzhou Hong, Mingyuan Zhang, Liang Pan, Zhongang Cai, Lei Yang, and Ziwei Liu. Avatar-CLIP: Zero-Shot Text-Driven Generation and Animation of 3D Avatars. *ACM Transactions on Graphics (TOG)*, 41(4):1–19, 2022.
- [9] Lianghua Huang, Di Chen, Yu Liu, Yujun Shen, Deli Zhao, and Jingren Zhou. Composer: Creative and controllable image synthesis with composable conditions. *arXiv preprint arXiv:2302.09778*, 2023.
- [10] Ajay Jain, Ben Mildenhall, Jonathan T Barron, Pieter Abbeel, and Ben Poole. Zero-Shot Text-Guided Object Generation With Dream Fields. In *Proceedings of the IEEE/CVF Conference on Computer Vision and Pattern Recognition*, pages 867–876, 2022.
- [11] Boyi Jiang, Yang Hong, Hujun Bao, and Juyong Zhang. Selfrecon: Self reconstruction your digital avatar from monocular video. In *Proceedings of the IEEE/CVF Conference on Computer Vision and Pattern Recognition*, pages 5605–5615, 2022.
- [12] Ruixiang Jiang, Can Wang, Jingbo Zhang, Menglei Chai, Mingming He, Dongdong Chen, and Jing Liao. AvatarCraft: Transforming Text into Neural Human Avatars with Parameterized Shape and Pose Control. *arXiv preprint arXiv:2303.17606*, 2023.
- [13] Wei Jiang, Kwang Moo Yi, Golnoosh Samei, Oncel Tuzel, and Anurag Ranjan. Neuman: Neural human radiance field from a single video. In *Computer Vision–ECCV 2022: 17th European Conference, Tel Aviv, Israel, October 23–27, 2022, Proceedings, Part XXXII*, pages 402–418. Springer, 2022.
- [14] Xuan Ju, Ailing Zeng, Chenchen Zhao, Jianan Wang, Lei Zhang, and Qiang Xu. HumanSD: A Native Skeleton-Guided Diffusion Model for Human Image Generation. *arXiv preprint arXiv:2304.04269*, 2023.
- [15] Chen-Hsuan Lin, Jun Gao, Luming Tang, Towaki Takikawa, Xiaohui Zeng, Xun Huang, Karsten Kreis, Sanja Fidler, Ming-Yu Liu, and Tsung-Yi Lin. Magic3D: High-Resolution Text-to-3D Content Creation. *arXiv preprint arXiv:2211.10440*, 2022.

- [16] Matthew Loper, Naureen Mahmood, Javier Romero, Gerard Pons-Moll, and Michael J Black. SMPL: a skinned multi-person linear model. *ACM transactions on graphics (TOG)*, 34(6):1–16, 2015.
- [17] Naureen Mahmood, Nima Ghorbani, Nikolaus F Troje, Gerard Pons-Moll, and Michael J Black. Amass: Archive of motion capture as surface shapes. In *Proceedings of the IEEE/CVF international conference on computer vision*, pages 5442–5451, 2019.
- [18] Gal Metzer, Elad Richardson, Or Patashnik, Raja Giryes, and Daniel Cohen-Or. Latent-NeRF for Shape-Guided Generation of 3D Shapes and Textures. *arXiv preprint arXiv:2211.07600*, 2022.
- [19] Ben Mildenhall, Pratul P Srinivasan, Matthew Tancik, Jonathan T Barron, Ravi Ramamoorthi, and Ren Ng. NeRF: Representing Scenes as Neural Radiance Fields for View Synthesis. *Communications of the ACM*, 65(1):99–106, 2021.
- [20] Nasir Mohammad Khalid, Tianhao Xie, Eugene Belilovsky, and Tiberiu Popa. CLIP-Mesh: Generating textured meshes from text using pretrained image-text models. In *SIGGRAPH Asia 2022 Conference Papers*, pages 1–8, 2022.
- [21] Alex Mohr and Michael Gleicher. Building efficient, accurate character skins from examples. *ACM Transactions on Graphics (TOG)*, 22(3):562–568, 2003.
- [22] Thomas Müller, Alex Evans, Christoph Schied, and Alexander Keller. Instant Neural Graphics Primitives with a Multiresolution Hash Encoding. *ACM Transactions on Graphics (ToG)*, 41(4):1–15, 2022.
- [23] Alex Nichol, Prafulla Dhariwal, Aditya Ramesh, Pranav Shyam, Pamela Mishkin, Bob McGrew, Ilya Sutskever, and Mark Chen. GLIDE: Towards Photorealistic Image Generation and Editing with Text-Guided Diffusion Models. *arXiv preprint arXiv:2112.10741*, 2021.
- [24] Alexander Quinn Nichol and Prafulla Dhariwal. Improved Denoising Diffusion Probabilistic Models. In *International Conference on Machine Learning*, pages 8162–8171. PMLR, 2021.
- [25] Ioannis Pantazopoulos and Spyros Tzafestas. Occlusion Culling Algorithms: A Comprehensive Survey. *Journal of Intelligent and Robotic Systems*, 35:123–156, 2002.
- [26] Georgios Pavlakos, Vasileios Choutas, Nima Ghorbani, Timo Bolkart, Ahmed AA Osman, Dimitrios Tzionas, and Michael J Black. Expressive body capture: 3d hands, face, and body from a single image. In *Proceedings of the IEEE/CVF conference on computer vision and pattern recognition*, pages 10975–10985, 2019.
- [27] Sida Peng, Junting Dong, Qianqian Wang, Shangzhan Zhang, Qing Shuai, Xiaowei Zhou, and Hujun Bao. Animatable neural radiance fields for modeling dynamic human bodies. In *Proceedings of the IEEE/CVF International Conference on Computer Vision*, pages 14314–14323, 2021.
- [28] Ben Poole, Ajay Jain, Jonathan T Barron, and Ben Mildenhall. DreamFusion: Text-to-3D using 2D Diffusion. *arXiv preprint arXiv:2209.14988*, 2022.
- [29] Alec Radford, Jong Wook Kim, Chris Hallacy, Aditya Ramesh, Gabriel Goh, Sandhini Agarwal, Girish Sastry, Amanda Askell, Pamela Mishkin, Jack Clark, et al. Learning Transferable Visual Models From Natural Language Supervision. In *International Conference on Machine Learning*, pages 8748–8763. PMLR, 2021.
- [30] Aditya Ramesh, Prafulla Dhariwal, Alex Nichol, Casey Chu, and Mark Chen. Hierarchical Text-Conditional Image Generation with CLIP Latents. *arXiv preprint arXiv:2204.06125*, 2022.
- [31] Robin Rombach, Andreas Blattmann, Dominik Lorenz, Patrick Esser, and Björn Ommer. High-Resolution Image Synthesis with Latent Diffusion Models. In *Proceedings of the IEEE/CVF Conference on Computer Vision and Pattern Recognition*, pages 10684–10695, 2022.

- [32] Chitwan Saharia, William Chan, Saurabh Saxena, Lala Li, Jay Whang, Emily Denton, Seyed Kamyar Seyed Ghasemipour, Burcu Karagol Ayan, S Sara Mahdavi, Rapha Gontijo Lopes, et al. Photorealistic Text-to-Image Diffusion Models with Deep Language Understanding. *arXiv preprint arXiv:2205.11487*, 2022.
- [33] Shunsuke Saito, Zeng Huang, Ryota Natsume, Shigeo Morishima, Angjoo Kanazawa, and Hao Li. Pifu: Pixel-aligned implicit function for high-resolution clothed human digitization. In *Proceedings of the IEEE/CVF international conference on computer vision*, pages 2304–2314, 2019.
- [34] Christoph Schuhmann, Romain Beaumont, Richard Vencu, Cade Gordon, Ross Wightman, Mehdi Cherti, Theo Coombes, Aarush Katta, Clayton Mullis, Mitchell Wortsman, et al. LAION-5B: An open large-scale dataset for training next generation image-text models. *arXiv preprint arXiv:2210.08402*, 2022.
- [35] Piyush Sharma, Nan Ding, Sebastian Goodman, and Radu Soricut. Conceptual Captions: A Cleaned, Hypernymed, Image Alt-text Dataset For Automatic Image Captioning. In *Proceedings of the 56th Annual Meeting of the Association for Computational Linguistics (Volume 1: Long Papers)*, pages 2556–2565, 2018.
- [36] Jiaming Song, Chenlin Meng, and Stefano Ermon. Denoising Diffusion Implicit Models. In *International Conference on Learning Representations*, 2021.
- [37] Jiaxiang Tang. Stable-dreamfusion: Text-to-3d with stable-diffusion, 2022. <https://github.com/ashawkey/stable-dreamfusion>.
- [38] Gusi Te, Xiu Li, Xiao Li, Jinglu Wang, Wei Hu, and Yan Lu. Neural capture of animatable 3d human from monocular video. In *Computer Vision–ECCV 2022: 17th European Conference, Tel Aviv, Israel, October 23–27, 2022, Proceedings, Part VI*, pages 275–291. Springer, 2022.
- [39] Haochen Wang, Xiaodan Du, Jiahao Li, Raymond A. Yeh, and Greg Shakhnarovich. Score Jacobian Chaining: Lifting Pretrained 2D Diffusion Models for 3D Generation. *arXiv preprint arXiv:2212.00774*, 2022.
- [40] Chung-Yi Weng, Brian Curless, Pratul P Srinivasan, Jonathan T Barron, and Ira Kemelmacher-Shlizerman. Humannerf: Free-viewpoint rendering of moving people from monocular video. In *Proceedings of the IEEE/CVF Conference on Computer Vision and Pattern Recognition*, pages 16210–16220, 2022.
- [41] Yuliang Xiu, Jinlong Yang, Xu Cao, Dimitrios Tzionas, and Michael J Black. ECON: Explicit Clothed humans Obtained from Normals. *arXiv preprint arXiv:2212.07422*, 2022.
- [42] Zhengming Yu, Wei Cheng, Xian Liu, Wayne Wu, and Kwan-Yee Lin. Monohuman: Animatable human neural field from monocular video. *arXiv preprint arXiv:2304.02001*, 2023.
- [43] Ailing Zeng, Xuan Ju, Lei Yang, Ruiyuan Gao, Xizhou Zhu, Bo Dai, and Qiang Xu. Deciwatch: A simple baseline for  $10\times$  efficient 2d and 3d pose estimation. In *Computer Vision–ECCV 2022: 17th European Conference, Tel Aviv, Israel, October 23–27, 2022, Proceedings, Part V*, pages 607–624. Springer, 2022.
- [44] Lvmin Zhang and Maneesh Agrawala. Adding Conditional Control to Text-to-Image Diffusion Models. *arXiv preprint arXiv:2302.05543*, 2023.